










T cell recognition of novel shared breast cancer antigens is frequently observed in peripheral blood of breast cancer patients

Nadia Viborg ^{a*}, Sofie Ramskov ^{a*}, Rikke Sick Andersen ^{b†}, Theo Sturm^c, Tim Fugmann ^{c‡},
Amalie Kai Bentzen ^a, Vibeke Mindahl Rafa^a, Per thor Straten ^{b,d}, Inge Marie Svane ^b, Özcan Met ^{b,d},
and Sine Reker Hadrup ^a

^aDepartment of Health Technology, Technical University of Denmark, Lyngby, Denmark; ^bCenter for Cancer Immune Therapy, Copenhagen University Hospital, Herlev, Denmark; ^cPhilochem AG, Otelfingen, Switzerland; ^dDepartment of Immunology and Microbiology, Faculty of Health and Medical Sciences, University of Copenhagen, Copenhagen, Denmark

ABSTRACT

Advances within cancer immunotherapy have fueled a paradigm shift in cancer treatment, resulting in increasing numbers of cancer types benefitting from novel treatment options. Despite originally being considered an immunologically silent malignancy, recent studies encourage the research of breast cancer immunogenicity to evaluate immunotherapy as a treatment strategy. However, the epitope landscape in breast cancer is minimally described, limiting the options for antigen-specific, targeted strategies. Aromatase, never in mitosis A-related kinase 3 (NEK3), protein inhibitor of activated STAT3 (PIAS3), and prolactin are known as upregulated proteins in breast cancer. In the present study, these four proteins are identified as novel T cell targets in breast cancer.

From the four proteins, 147 peptides were determined to bind HLA-A*0201 and -B*0702 using a combined *in silico/in vitro* affinity screening. T cell recognition of all 147 peptide-HLA-A*0201/-B*0702 combinations was assessed through the use of a novel high-throughput method utilizing DNA barcode labeled multimers.

T cell recognition of sequences within all four proteins was demonstrated in peripheral blood of patients, and significantly more T cell responses were detected in patients compared to healthy donors for both HLA-A*0201 and -B*0702. Notably, several of the identified responses were directed toward peptides, with a predicted low or intermediate binding affinity. This demonstrates the importance of including low-affinity binders in the search for epitopes within shared tumor associated antigens (TAAs), as these might be less subject to immune tolerance mechanisms.

The study presents four novel TAAs containing multiple possible targets for immunotherapy of breast cancer.

ARTICLE HISTORY

Received 10 April 2019
Revised 29 August 2019
Accepted 30 August 2019

KEYWORDS

Breast cancer; breast cancer immunogenicity; tumor associated antigens; TAAs; TAAs in breast cancer; shared tumor antigens; overexpression antigens; immunomonitoring; tumor specific CD8+ T cells; tumor specific cytotoxic T cells


Introduction

Throughout the last decade, the remarkable progress in the field of cancer immunotherapy has resulted in a paradigm shift in cancer treatment, establishing immunotherapy as the fourth pillar of treatment, next to conventional therapies; surgery, radiation, and chemotherapy. Unprecedented improvements of response rate and overall survival have been shown for an increasing range of cancer types, with various forms of immunotherapy.

Breast cancer remains the largest group of female cancers and a major cause of death, despite improvements in time of diagnosis and range of treatment options.^{1,2} Although generally considered to be poorly immunogenic, an increasing body of evidence points to a role of immunotherapy in breast cancer, especially in triple negative breast cancer, the subtype

where other treatment options are extremely limited.³ In recent years, a major focus of immune therapy has been on mutation-derived neo-antigens, with mutational burden and predicted number of neo-antigens shown to correlate with favorable clinical outcome and benefit from immune check-point therapy.⁴⁻⁶

However, the burden of somatic mutations varies greatly between tumor types,⁷ as do the chances of identifying patient-specific targetable neo-antigens, to which effector cells of the immune system can be actively directed. Breast cancers are among low mutational burden tumors and although a recent study demonstrated the presence of neo-antigen reactive T cells in tumor infiltrating lymphocytes (TILs) used to treat a breast cancer patient who obtained a complete durable regression,⁸ we would argue that the group of shared tumor associated antigens (TAAs) may play an additional role in this cancer type. TAAs are


CONTACT Sine Reker Hadrup  sirha@dtu.dk  Section for Experimental and Translational Immunology, Department of Health Technology, Technical University of Denmark, Kemitorvet Building 204, 2800 Kgs, Lyngby, Denmark

*These authors contributed equally

†Current affiliation: Department of Pathology, Odense University Hospital, Odense, Denmark

‡Current affiliation: Max Delbrück Center for Molecular Medicine, Berlin, Germany

This article has been republished with minor changes. These changes do not impact the academic content of the article.

 Supplemental data for this article can be accessed [publisher's website](#).

© 2019 The Author(s). Published with license by Taylor & Francis Group, LLC.

This is an Open Access article distributed under the terms of the Creative Commons Attribution-NonCommercial-NoDerivatives License (<http://creativecommons.org/licenses/by-nc-nd/4.0/>), which permits non-commercial re-use, distribution, and reproduction in any medium, provided the original work is properly cited, and is not altered, transformed, or built upon in any way.

of value both in the antigen-defined treatment setting, where they can act directly as targets of therapy, as well as in the antigen-undefined setting, where they can be used for immunomonitoring and potentially be able to predict treatment outcome.⁹ Few breast cancer-specific TAAs are known; those that have already been described (e.g. HER2¹⁰ and MUC1¹¹) are only expressed in subgroups of patients; and when used in vaccines, they have shown limited clinical activity, albeit modest immunological activity.² Therefore, there is an unmet need for identification of TAAs in breast cancer.

In this study we investigate aromatase, prolactin, never in mitosis A-related kinase 3 (NEK3) and protein inhibitor of activated signal transducer and activator of transcription 3 (PIAS3) as possible TAAs in breast cancer. Aromatase is the key enzyme in estrogen synthesis and is a heterodimer composed of the ubiquitously expressed flavoprotein NADPH-cytochrome P450 reductase and aromatase cytochrome P450.¹² Aromatase inhibitors are already successful in treating breast and other female cancers, underlining the relevance of investigating aromatase as a TAA.¹³ Prolactin and two of its downstream intracellular signaling proteins, NEK3 and PIAS3, are involved in breast lobulo-alveolar expansion and differentiation prior to milk synthesis and secretion.^{14,15} All four proteins have been described to have an increased expression in breast cancer compared to healthy breast tissue.^{12–16}

Results

Peptides were selected based on a combined *in silico* and *in vitro* selection pipeline

The four proteins aromatase, NEK3, PIAS3, and prolactin were selected for investigation based on a literature search, prioritizing proteins that fulfilled criteria of tissue restriction and increased expression in malignant compared to healthy breast tissue (Table 1). Aromatase mRNA levels have been shown to be significantly increased in breast cancer compared to healthy breast tissue, e.g. in a study by Harada, where mRNA levels were significantly elevated ($p < 0.01$).¹⁶ Likewise, significantly increased expression of prolactin, and the two intracellular signaling proteins, NEK3 and PIAS3, have been demonstrated in breast tumor tissue using immunohistochemistry staining. This revealed a significant difference in expression between

normal/hyperplastic epithelium and ductal carcinoma *in situ*/invasive carcinoma (t-tests, all p values < 0.02).¹⁴

Expression of all four proteins was validated in two breast ductal carcinoma cell lines (BT-549 and HCC1937), as well as in two breast adenocarcinoma cell lines (EFM-192A and MDA-MB-231) (Supplementary Figure S1). MHC class I presentation of peptides from the four proteins was investigated by mass spectrometry analysis and demonstrated presentation of peptides from PIAS3 in three of three tested cell lines (Supplementary Figure S1, Supplementary Table S3).

A library of peptides was generated based on a two-step *in silico* + *in vitro* selection process (Table 2, Supplementary Table S2). In the initial *in silico* prediction step, two available computational pipelines, SYFPEITHI and NetMHC 3.0, were used for predicting the MHC class I binding affinity of the individual peptides in the selected proteins. We identified potential HLA-A*0201 and -B*0702 binding 9- and 10-mer peptides within the sequences of the four proteins. The number of predicted peptides out of total possible peptides from each protein sequence correlated with the size of the protein, as would be expected. 415 of the total 3644 peptides were predicted with selection cut offs set to accommodate inclusion of both high and low affinity HLA-A*0201 and -B*0702 ligands (SYFPEITHI: ≥ 19 , NetMHC 3.0: ≤ 1000 nM), given that the proteins of interest are shared antigens. Previous analyses have demonstrated very low affinity epitopes of relevance in shared antigens.^{17, 18} As such, the binding of the predicted peptides was experimentally tested *in vitro* with an MHC ELISA.¹⁹ 147 of the 415 *in silico* predicted peptides were selected for further analysis, based on 50% (A*0201) and 70% (B*0702) binding affinity, compared to a reference of high affinity virus-derived ligands (Table 2, Supplementary Table S2).

Table 2. Peptide selection from the four proteins through a combined *in silico* prediction and *in vitro* binding assay.

Protein	Size (amino acids)	Total number of peptides (9- and 10-mers)	<i>In silico</i> predicted peptides ^a (9- and 10-mers)	<i>In vitro</i> selected peptides ^b (9- and 10-mers)
Aromatase	503	989	141	49
NEK3	506	995	85	36
PIAS3	628	1239	148	50
Prolactin	227	437	41	12
Total		3644	415	147

^a*In silico* prediction cut offs: SYFPEITHI score ≥ 19 and/or NetMHC 3.0 IC50 ≤ 1000 nM.

^b*In vitro* binding cut offs: A*0201: 50% of CMV control, B*0702: 70% of CMV control.

Table 1. Overview of protein targets selected for investigation as tumor associated antigens.

Protein	Full name	Normal function	Role in breast cancer	Normal expression	Increased expression	Reference
Aromatase	Aromatase	Key enzyme in estrogen synthesis. Heterodimer composed of aromatase cytochrome P450 and NADPH-cytochrome P450 reductase ^a	Enhanced tumor cell growth	Breast, ovary, testes, adipose tissue, skin, hypothalamus, placenta	Breast, endometrial & ovarian cancer	12,13,16
NEK3	Never in mitosis A-related kinase 3	Prolactin receptor-associated protein, positive regulator	Enhanced survival, motility, and invasion of tumor cells	Ubiquitous	Breast, colorectal, carcinoid & testicular cancer	14
PIAS3	Protein inhibitor of activated STAT3	Prolactin receptor-associated protein, negative regulator	Induction of malignant transformation	Ubiquitous	Breast cancer, glioma	14
Prolactin	Prolactin	Growth and differentiation hormone	Enhanced breast epithelial survival and motility, inhibition of tumor cell apoptosis	Breast, brain (pituitary gland), placenta, endometrium	Breast cancer	14,15

^aOnly aromatase cytochrome P450 is investigated in this study.

All peptides were predicted with the 3.0 version of NetMHC. However, at the time of publication, a new version had been developed (NetMHCpan 4.0). Therefore, we conducted a comparison of the prediction output from the current library of the two database versions (Supplementary Figure S2). The outputs from the two different versions of NetMHC correlated tightly, with only few outliers representing a difference in predicted affinity between the two databases.

Significantly more TAA-specific T cell responses were detected *ex vivo* in peripheral blood from breast cancer patients than in healthy donors

The 147 predicted breast cancer TAA peptides were synthesized and used to generate individual peptide MHC (pMHC) monomers with UV-mediated peptide exchange as previously described.¹⁹ We then multimerized the pMHC monomers onto a PE-labeled polysaccharide backbone, coupled to a DNA barcode, unique to each specific pMHC (as described in²⁰). We included 10 epitopes from common viruses; influenza virus (FLU), Epstein-Barr virus (EBV), or cytomegalovirus (CMV) epitopes. This yielded 157 different pMHC multimers that were used to stain cryopreserved peripheral blood from breast cancer patients (Patient cohort 1, $n = 25$) and healthy donors (Healthy Donor cohort 1, $n = 17$). Based on flow cytometry, we sorted for CD8⁺ T cells with the ability to bind to pMHC multimers, the associated DNA barcodes were amplified and the specificity of the CD8⁺ T cells could be revealed by sequencing of the DNA barcodes. T cell responses were defined as any pMHC complex enriched in the sorted T cell fraction with $p < 0.001$ (FDR < 0.1%).

We observed significantly more TAA-specific T cell responses in patient samples than in healthy donors (Figure 1(a,b)) (Fischer's exact test, A*0201: $p < 0.0001$, B*0702: $p = 0.03$). Of the total 66 TAA-specific T cell responses detected, only one did not match the HLA of the donor (sample P1.2 response to

A*0201 restricted ARO9(444) peptide). With limited patient sample material, it was particularly advantageous to screen for all multimer specificities in parallel. Across 17 healthy donors, we detected numerous T cell responses directed toward virus-derived epitopes, validating the technical feasibility and general immune competence of the healthy donor population. Yet, a minor difference was observed between immune recognition of virus-derived epitopes in patients and healthy donors.

TAA-specific T cell responses were validated by specific expansion and cluster in immunological hotspots

To validate TAA-specific T cell responses, we specifically expanded T cells from PBMCs, based on the responses observed by the DNA barcoded pMHC multimer screening. Antigen-specific T cells were stimulated using the given pMHC complex, together with a cytokine cocktail. Following this strategy, we observed T cell responses with frequencies >1% of CD8⁺ T cells detected by multimer staining, directed toward prolactin- and NEK3-derived peptides (Figure 2(a,b)). Additionally, for a subset of breast cancer samples, we enriched for TAA-restricted T cells by magnetic bead sorting, using the entire pMHC multimer library with all 147 peptide specificities. After magnetic bead enrichment, samples were analyzed by DNA barcoded pMHC multimer screening. With this strategy, a number of responses were confirmed and a number of additional responses were detected (Supplementary Figure S3(a)).

In a verification cohort of breast cancer patient samples (Patient cohort 2, $n = 18$) and healthy donors (Healthy Donor cohort 2, $n = 13$), T cell reactivity was detected in peripheral blood against the same TAAs. Samples in Patient cohort 2 and Healthy Donor cohort 2 were screened for T cell reactivity with a fluorescently labeled combinatorial-encoded pMHC multimer library *ex vivo*, and after enrichment by magnetic bead sorting. In the verification cohort, T cell responses were distributed across the four proteins (Supplementary Figure S3

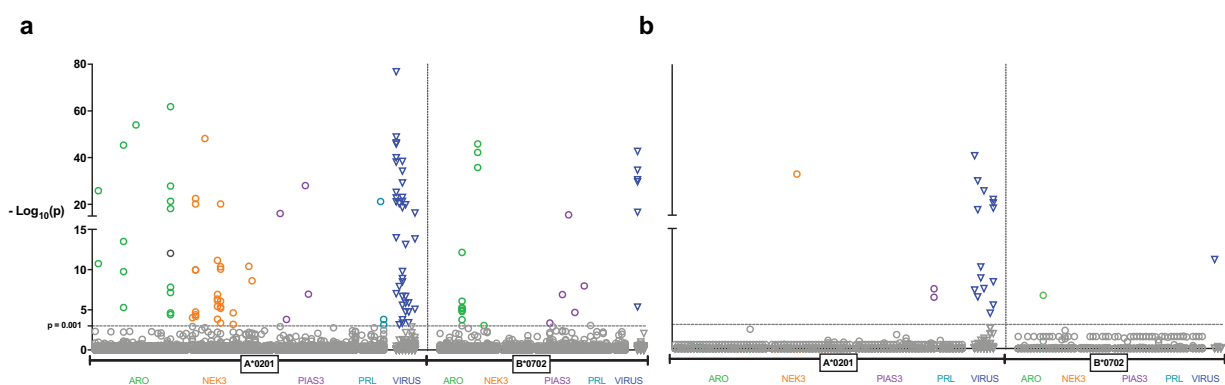


Figure 1. Detection of T cell responses to potential breast cancer TAAs and virus derived peptides.

Screening for T cell recognition by DNA barcoded pMHC multimers in peripheral blood directly *ex vivo* of 25 breast cancer patients in Patient cohort 1 (a) and 17 healthy donors in Healthy Donor cohort 1 (b). Left side, T cell responses to HLA-A*0201 restricted peptides (90 breast cancer derived peptides and 7 virus derived peptides). Right side, T cell responses to HLA-B*0702 restricted peptides (57 breast cancer derived peptides and 3 virus derived peptides). Colored circles represent T cell responses to aromatase (green), NEK3 (orange), PIAS3 (purple), and prolactin (turquoise) derived peptides. Dark blue triangles represent T cell responses to virus peptides from influenza virus, Epstein-Barr virus, or cytomegalovirus epitopes. Dark gray circle above dotted line represents HLA-A*0201 restricted response detected in a patient that is not A*0201 by HLA typing. All points lying on the same vertical axis implies multiple T cell responses to the same peptide across several donors. Data plotted on the y-axis as $-\log_{10}(p)$ of the relevant pMHC-associated DNA barcode. The horizontal dotted line represents the detection limit ($p = 0.001$ /FDR = 0.1) determining a T cell responses and all dots below are not considered as T cell responses.

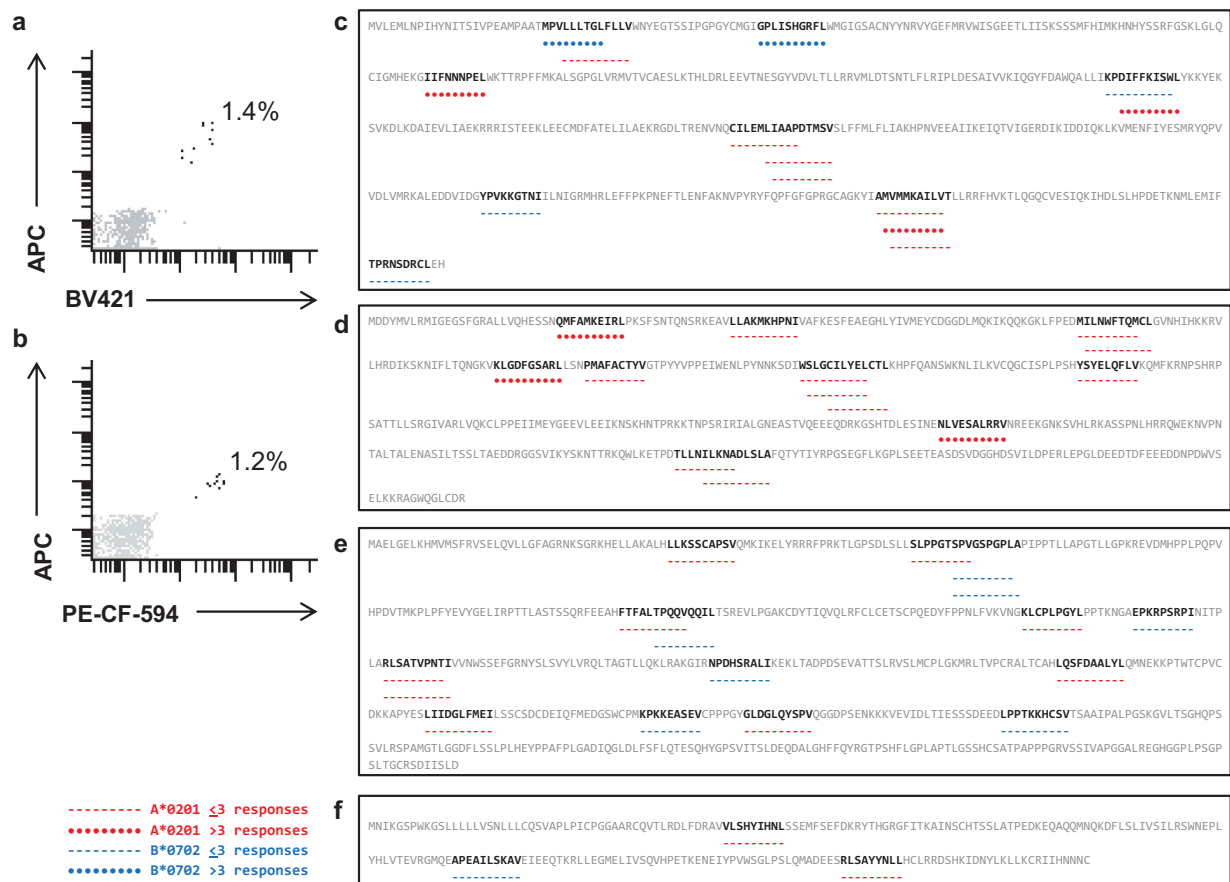


Figure 2. Validation of TAA directed T cell recognition and immunological hotspots in breast cancer antigens.

(a–b), pMHC directed expansion of T cells validated the presence of (a), A*0201 PRL9(52) specific T cells in Patient P1.8 and (b), A*0201 NEK10(329) specific T cells in Patient P1.9 from Patient cohort 1. Frequencies of pMHC multimer specific T cells out of total CD3+ CD8+ TILs are displayed.

(c–f), Protein sequences of Aromatase (c), NEK3 (d), PIAS3 (e) and prolactin (f), with immunological hotspots illustrated. Peptide sequences, for which T cell recognition was detected in Patient cohorts 1 & 2 are marked with red dashes (A*0201, < 3 responses), red dots (A*0201, > 3 responses), blue dashes (B*0702, < 3 responses), and blue dots (B*0702, > 3 responses).

(b), Supplementary Table S2) and were preferentially observed in breast cancer patients, as opposed to healthy donors.

All TAA-specific T cell responses detected directly *ex vivo* and following pMHC-specific expansion in Patient cohort 1 and 2 were mapped to their specific positions along the length of the protein sequence (Figure 2(c–f)). This analysis revealed that epitopes giving rise to T cell responses tended to cluster, indicating potential “immunological hotspots”. Evidently, the immunological hotspots covered certain regions of the protein sequences where several T cell epitopes overlapped. Furthermore, multiple T cell responses were observed toward the same epitopes and overlapping regions across multiple breast cancer patient samples, and with restriction to both HLA-A*0201 and –B*0702.

Each of the four investigated proteins contained targets of TAA-specific T cells

T cell reactivity detected in peripheral blood from breast cancer patients and healthy donors was distributed across the four proteins, with most responses toward aromatase- and NEK3-derived peptides (Figure 3(a)). In blood from

healthy donors, the number of T cell responses was significantly lower than in breast cancer patients for aromatase- and NEK3- derived peptides, and no T cell reactivity was detected toward prolactin-derived peptides. With regards to specific epitope count, it is evident that for several T cell epitopes in aromatase and NEK3, T cell reactivity was detected multiple times throughout a range of screened patients (8 unique epitopes detected for each protein, covered by 28 and 27 individual T cell responses). For PIAS3 and prolactin, the epitopes found were more unique for each donor, with less overlap in detection of the same T cell response across several samples (11 and 2 unique epitopes, respectively, covered by 12 and 3 individual T cell responses, respectively). Each protein gave rise to a similar fraction of epitopes (16–22%) when relating the number of T cell epitopes to the number of HLA binding peptides, i.e. screened for T cell recognition within each protein.

Peptides were divided into two groups, based on detection of T cell responses (response \pm), to investigate potential differences in characteristics of immunogenic versus non-immunogenic peptides in this context. First, evaluating the pMHC affinity predicted by NetMHCpan 4.0 and shown as

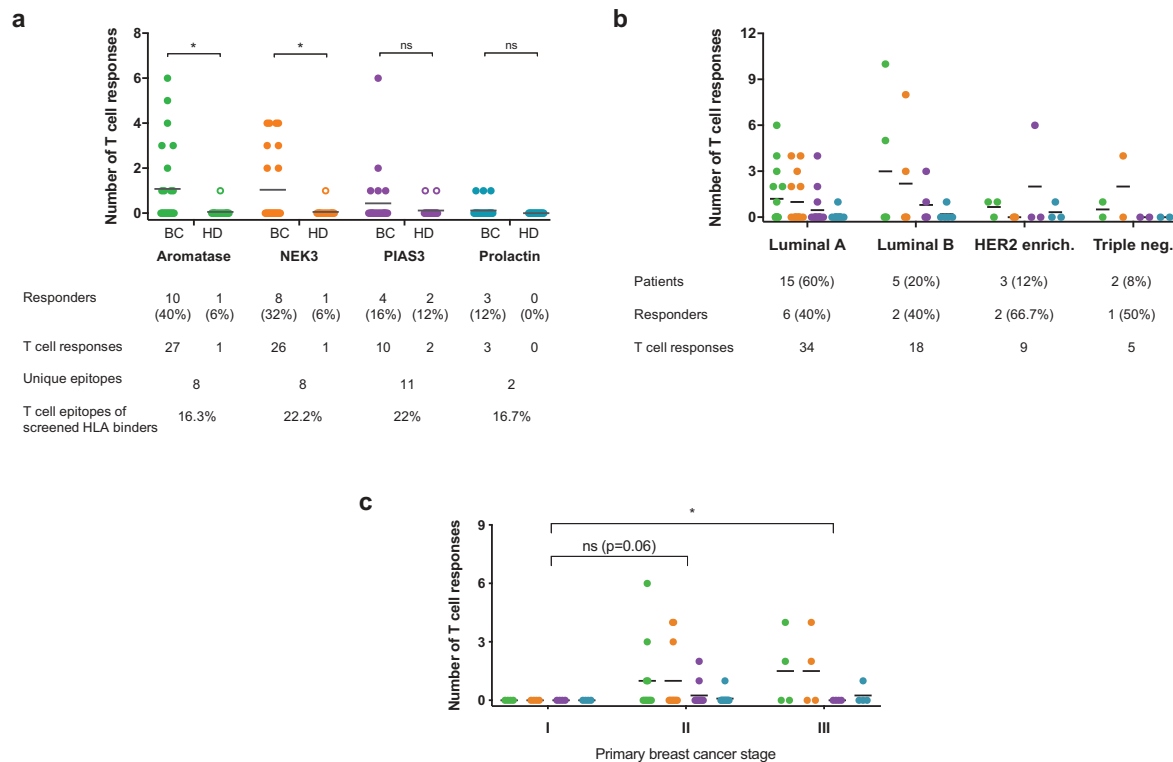


Figure 3. Distribution of detected T cell responses by protein and breast cancer subtype or stage.

Plots display distribution of T cell responses detected in breast cancer Patient cohort 1 and Healthy Donor cohort 1 *ex vivo*. (a), T cell response distribution across the four potential TAAs; aromatase (green), NEK3 (orange), PIAS3 (purple), and prolactin (turquoise). (b), Distribution of TAA specific T cell responses observed in breast cancer patients separated by breast cancer subtypes. (c), Distribution of TAA specific T cell responses observed in breast cancer patients by staging of primary tumor. Asterisks indicate significance levels (*, $p < 0.05$), nonparametric Mann-Whitney test.

nM binding affinity and % eluted ligand Rank (Supplementary Figure S4(a–b)). Second, stability was predicted by NetMHCStabpan 1.0 and shown as %Rank (Supplementary Figure S4(c)). There were no significant differences in mean predicted affinity or stability between peptides, yielding a T cell response (+) or not (-).

T cell reactivity toward breast cancer TAAs occurs independently of cancer subtype and disease stage

Breast cancer patients in cohort 1 were stratified into different molecular subtypes based on pathological examination of tumors (Supplementary Table S1). Four major subtypes of breast cancer are commonly described based on tumor cell expression of hormone receptors (estrogen receptor; ER, and progesterone receptor; PR) and growth factor HER2 as follows: luminal A (ER+ and/or PR+, HER2⁻), luminal B (ER+ and/or PR+, HER2+), HER2 enriched (ER⁻ and PR⁻, HER2+), and triple negative (ER⁻, PR⁻, HER2⁻). Breast cancer patients with TAA-specific T cell responses were observed for all subtypes and there seemed to be no preferential distribution for any particular subtype in the investigated patient cohort (Figure 3(b)). However, for certain subtypes, i.e. HER2 enriched and triple negative, the number of patients included is <5, and hence too few to firmly evaluate for potential differences.

For 20 out of 25 breast cancer patients from cohort 1 it was possible to determine disease stage based on UICC TNM

guidelines (Supplementary Table S1). Interestingly, TAA-specific T cell responses were observed in blood from patients at disease stage II and III, and none in blood from patients at stage I, with significantly more responses in disease stage III than disease stage I (Figure 3(c)). This interesting observation from a relatively small cohort of patients at each stage (I: 4 patients, II: 12 patients, and III: 4 patients), could indicate enhanced T cell reaction with higher tumor burden or metastatic disease, but such findings should be validated in a larger cohort.

Breast cancer TAA-specific T cells have functional capacity upon stimulation

To assess the functional capacity of TAA-responsive T cells in patients, we combined the DNA barcoded pMHC multimer screening with measuring cytokine production by intracellular staining, as previously described.²⁰ A selection of PBMCs from Patient cohort 1 were stimulated with 1) a pool of TAA peptides specific for each patient sample, selected based on T cell responses found by multimer screening of *ex vivo* or enriched material, or 2) a mixture of HLA matching breast cancer cell lines (BT-549, HCC1937, EFM-192A and MDA-MB-231). After stimulation, cells were stained and analyzed simultaneously for functional reactivity and T cell specificity by sorting T cells solely based on their cytokine secretion profile, IFN γ and/or TNF α secretion (ICS^{pos}) or no cytokine secretion (ICS^{neg}), after which

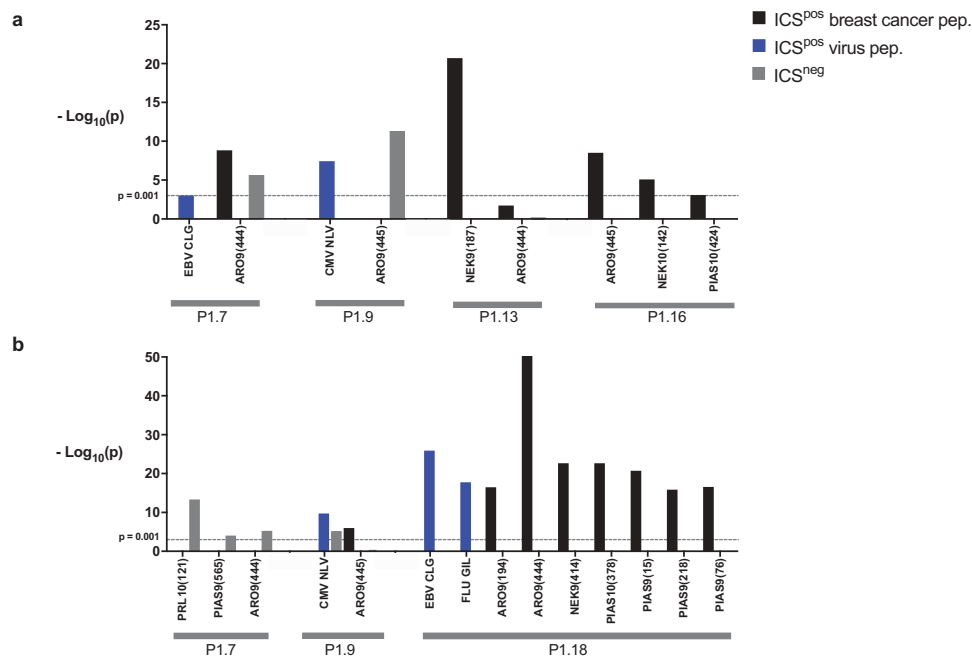


Figure 4. Functional assessment of breast cancer TAA responsive T cells.

Bar plots representing the parallel assessment of T cell specificity and functional responsiveness of breast cancer patient PBMCs from Patient cohort 1. PBMCs were stimulated with a patient specific peptide pool (a) or breast cancer tumor cell lines (b), stained with INF γ and TNF α antibodies and with DNA barcoded pMHC multimers. CD8+ T cells were sorted based on production of INF γ and/or TNF α (ICS^{Pos}) versus no production of these cytokines (ICS^{Neg}). pMHC multimer binding was not included as sorting criteria. Data plotted as $-\text{Log}_{10}(p)$ of the relevant pMHC associated DNA barcode. The dotted lines represents the detection limit ($p = 0.001/\text{FDR} = 0.1$) and all bars below are not considered as T cell responses. Black bars represent T cell responses detected toward breast cancer derived peptides, blue bars represent T cell responses detected toward virus derived peptides, both in the ICS^{Pos} fraction, whereas gray bars represent T cell responses detected in the ICS^{Neg} fraction.

sequencing of the pMHC associated DNA barcode uncovered the antigen specificity of the sorted T cell populations.

Patient samples stimulated with peptide pools showed presence and functional capacity of T cells specific for aromatase, NEK3, and PIAS3 peptides (Figure 4(a)). Recognition of two peptides from aromatase with overlapping sequences (ARO9 (445) and ARO9 (444), both restricted to HLA-A*0201) were present across most samples and cytokine-producing in some. Relevant virus-derived peptides were included for stimulation, with detection primarily in ICS^{Pos} T cells. Stimulation with tumor cell lines showed T cells specific for all investigated TAAs, but with only functional capacity for aromatase, NEK3, and PIAS3 peptides (Figure 4(b)). Patient P1.7 had TAA-specific T cells in the ICS^{Neg} T cell fraction, whereas patient P1.18 had multiple TAA-specific T cells in the ICS^{Pos} T cell fraction.

Discussion

Herein, we present the detection of CD8+ T cell responses toward peptides derived from breast cancer associated antigens. The ambition was to identify peptides from proposed breast cancer TAAs aromatase, NEK3, PIAS3, and prolactin, and validate them as T cell epitopes. This was accomplished by screening a cohort of 25 breast cancer patient samples and 17 healthy donor samples for recognition of 147 selected peptides restricted to HLA-A*0201 and -B*0702. In the primary cohort, significantly more CD8+ T cell responses were observed in breast cancer patient samples than healthy donor samples. This was uncovered by a high throughput DNA-barcode label pMHC multimer

screening; a method which enabled the investigation of hundreds of breast cancer-specific CD8+ T cells in parallel. The same strategy was recently employed to identify autoreactive T cells in narcolepsy.²¹ Our findings were confirmed in a verification cohort (18 patients, 13 healthy donors) by fluorochrome labeled pMHC multimers, where again CD8+ T cell responses to the breast cancer-derived peptides were overrepresented in patient samples versus healthy donors. Our findings across two cohorts and two technological screening platforms show strong evidence that the four investigated proteins contain CD8+ T cell targets.

Strikingly, epitopes were shared between patients, overlapped for HLA*A0201 and -B*0702 and tended to cluster along the length of the protein sequences, indicating the presence of immunological hotspots. Importantly, upon inspection of *in silico* predicted properties of peptides \pm CD8+ T cell recognition, it was evident that immunogenic peptides were not significantly better binders or more stable in the MHC complex than non-immunogenic peptides. This emphasizes the importance of evaluating the inclusion criteria when selecting peptides for T cell screening endeavors. As indicated in this study, particularly when the targets are of shared origin and the matching T cells therefore subject to stricter selection during development in the thymus, the need for including intermediate or even low affinity binders is of importance.

Several of the *ex vivo* observed CD8+ T cell responses were verified after *in vitro* expansion, with expanded responses from two patient samples validated by fluorescently-labeled pMHC multimer staining. In addition to observing CD8+ T cell responses *ex vivo*, and after specific expansion, a subset of breast cancer patient samples were further investigated for functional

capacity upon stimulation and ICS. Interestingly, the functional analysis revealed breast cancer patient CD8+ T cell reactivity to some of the TAA-derived peptides that were observed in *ex vivo* screenings. A limitation of the study is the lack of patient autologous tumor cells. Although we document T cell recognition of allogeneic, commercially available cancer cell lines, the pairing of patient T cells and autologous tumor cell lines would enable verification of autologous recognition. The same limitation applies to the mass spectrometry analysis, where MHC class I expression of peptides from all four proteins was investigated in three commercially-available breast cancer cell lines. Here one putative HLA-A*02:01 ligand (PIAS3; SIVAPGGAL) identified by mass spectrometry was overlapping with the T cell screening peptide library. This peptide did not result in T cell responses. Despite the limited overlap, the detection of four MHC class I embedded PIAS3 peptides does document expression and antigen-processing of PIAS3 in breast cancer.

Though breast cancer was originally considered an immunologically silent malignancy, the data reported herein and recent publications from others encourage further research of immunogenicity of breast cancer.^{22–24} In the current era of neo-epitopes and a strong focus on personalized strategies, the breast cancer TAAs investigated here provide a broader approach with potential applicability across many patients. Of note, the present study focused on HLA-A*0201 and – B*0702, where there was already some sequence-overlap between epitopes observed. Expanding the analysis to additional HLA alleles would enable coverage of a greater part of the population and possibly strengthen the tendency of immunological hotspots. For therapeutic use, the existence of immunological hotspots suggests a compelling approach, where patients could be vaccinated with a long peptide spanning a hotspot, regardless of HLA status. Such an “off-the-shelf” antigen could possibly provide an add-on to more personalized approaches, targeting e.g., neo-epitopes. Notably, we found TAA-specific T cell responses in all breast cancer subtypes suggesting that a therapy based on targeting these antigens could benefit many patients. Furthermore, TAA-specific T cell responses seem to be enhanced at more advanced stages of disease, indicating that at an early stage of breast cancer development, where tumor size is small and there is no spread to lymph nodes, these tumors are less immunogenic. Also this finding argues for enhancement of T cell reactivity by boosting the tumor specific T cells in both frequency and functionality, e.g. through checkpoint inhibition. Identification and understanding of T cell epitopes can contribute to diagnostics, immunomonitoring, and immunotherapy in cancer patients. This study provides an important contribution of four novel TAAs containing multiple epitopes in a poorly described landscape of breast cancer antigens and encourages further investigation of aromatase, NEK3, PIAS3 and prolactin in a preclinical setting, e.g. assessment of expression and immunogenicity in mouse models.

Materials and methods

Patient and healthy donor samples

Breast cancer patient samples were kindly provided by the Department of Oncology and the Center for Cancer Immune Therapy, Herlev Hospital, Denmark, with approval by the

regional ethics committee for the Capital Region of Denmark. Breast cancer patient samples came from two different cohorts, as listed in Supplementary Table S1. All patient blood samples in cohort 1 were drawn at the time of primary diagnosis, before any treatment was initiated. Patients in cohort 2 were untreated, or treated with one or more standard therapies (chemo-, radiation and endocrine), but did not receive immunotherapy prior to blood sampling. Healthy donor samples were collected by approval of the local Scientific Ethics Committee, with donor written informed consent obtained according to the Declaration of Helsinki. Healthy donor blood samples were obtained from the blood bank at Rigshospitalet, Copenhagen, Denmark. All samples were obtained anonymously.

PBMC isolation from whole blood

Peripheral blood mononuclear cells (PBMCs) from breast cancer patients and healthy donors were obtained from whole blood with density centrifugation on Lymphoprep (Axis-Shield PoC, Cat#1114544) in Leucosep tubes (Greiner Bio-One, Cat#227288) and cryopreserved at -150°C in FCS (fetal calf serum, Gibco, Cat#10500064) + 10% DMSO (dimethyl sulfoxide, Sigma-Aldrich, Cat#C6164).

HLA tissue typing

HLA class I tissue typing was determined by either flow cytometry with anti-HLA-A*02 (Abcam, Cat#ab27728) and anti-HLA-B*07 antibodies (Abcam, Cat#ab33331), PCR, or by high-resolution next generation sequencing (IMGM, Martinsried, Germany).

Tumor cell lines

Breast cancer cell lines were kindly provided by the Center for Cancer Immune Therapy, Herlev Hospital, Denmark (BT-549 and MDA-MB-231) or purchased from ATCC (HCC1937, Cat#CRL-2336) and DSMZ (EFM192A, Cat#ACC258) and grown in R10 (RPMI + GlutaMAXTM, Gibco, Cat#61870010 + 10% FCS) including 1% penicillin-streptomycin (P/S, Sigma-Aldrich, Cat#P0781).

Expression of TAAs by tumor cell lines

Expression of proteins aromatase, NEK3, PIAS3, and prolactin was investigated in breast cancer cell lines BT-549, EFM192A, HCC1937, and MDA-MB-231 by intracellular staining with anti-aromatase (Bioss, Cat#bs-1292R), anti-NEK3 (Abcam, Cat#83221), anti-PIAS3 (Abcam, Cat#ab77231) and anti-prolactin (Lifespan Biosciences, Cat#LS-C209024) antibodies, with analysis by flow cytometry. Tumor cells were harvested and washed twice in R10, once in PBS + 2% FCS. Thereafter, cells were permeabilized and fixated with the Transcription Factor Buffer Set (BD, Cat#562574) and stained for 30 min at 4°C with specific antibodies or isotype/stain control antibodies. Followingly, cells were washed twice in PBS + 2% FCS and stained with secondary antibodies when relevant, washed twice in PBS + 2% FCS and finally fixated in 1% paraformaldehyde (PFA, Santa Cruz Biotechnology, Cat#sc-281692) until analysis.

Endogenous peptide presentation on tumor cell lines

The endogenous MHC class I immunopeptidomes of the breast cancer cell lines BT-549, EFM-192A and MDA-MB-231 were analyzed by MHC immunoaffinity chromatography (MHC-IAC) followed by liquid chromatography-mass spectrometry (LC-MS) as detailed in Supplementary Methods. Briefly, each cell line was subjected to two parallel MHC-IACs using 108 cells per analysis and employing the W6/32 antibody. Peptides were measured at a Q Exactive (Thermo Scientific) using a top 10 data dependent acquisition strategy, and data were processed with Proteome Discoverer version 1.4 employing Sequest HT and Percolator to achieve a false discovery rate of 5%.

In silico HLA-A*0201 and -B*0702 binding affinity and stability prediction of peptides

The binding affinity and stability to HLA-A*0201 and HLA-B*0702 of 9- and 10- amino acid peptides from the four investigated proteins were predicted by SYFPEITHI,²⁵ NetMHC 3.0,²⁶ NetMHCpan 4.0²⁷ and NetMHCstabpan 1.0.²⁸ Peptides with a binding score ≥ 19 in SYFPEITHI and/or ≤ 1000 nM in NetMHC 3.0 were analyzed.

Peptides

All breast cancer associated and virus-derived peptides were purchased from Pepscan (Pepscan Presto BV, Lelystad, Netherlands) and dissolved to 10 mM in DMSO. A full list of breast cancer associated peptides used in the study can be found in Supplementary Table S2. The following virus-derived peptides were included in the study; HLA-A*0201 restriction: CMV pp65 (NLVPMVATV), CMV IE1 (VLEETSVML), EBV BMF1 (GLCTLVAML), EBV BRLF1 (YVLDHLIVV), EBV LMP2 (CLGGLTMV), EBV LMP2 (FLYALALL), FLU MP (GILGFVFTL), HIV pol (ILKEPVHGV), HLA-B*0702 restriction: CMV pp65 (RPHERNGFTV), CMV pp65 (TPRVTGGGAM), EBV EBNA (RPPFIRLL).

In vitro affinity testing and selection of peptides

The experimental binding of *in silico* predicted peptides was assessed by MHC ELISA, as previously described by Rodenko et al.¹⁹ Briefly, biotinylated peptide-HLA (pHLA)-A*0201/B*0702 complexes were generated by UV-mediated peptide exchange and incubated on streptavidin (Invitrogen, Cat#S888)-coated Maxisorp plates (NUNC, Cat#44-2404-21) for 1 h at 37°C. The pHLA complexes were then incubated with horseradish peroxidase-conjugated β_2 microglobulin (β_2m) antibody (Acris GmbH, Cat# 604HRP) for an additional 1 h at 37°C, binding only to correctly folded peptide-MHC (pMHC) molecules. Plates were washed and a colorimetric reaction was initiated by the addition of tetramethylbenzidine peroxidase substrate (KPL, Cat#506606). Finally, the optical density (OD) of each well was measured at 405 nm by an ELISA reader (Epoch microplate spectrophotometer, Bio-Tek) and values were normalized to the OD

of a CMV-derived virus peptide with a known high binding affinity by the formula,

$$\text{Index value} = \frac{OD_{\text{peptide}} - OD_{\text{PBS}}}{OD_{\text{CMVcontrol peptide}}}$$

HLA-binding peptides were selected based on their ability to rescue the A*0201/B*0702 molecule from degradation after UV-mediated cleavage of the conditional ligand and compared to that of a CMV virus-derived control with known high binding affinity. The threshold for selection was set at 50% (A*0201) and 70% (B*0702) of the binding affinity of the respective virus-derived peptides.

MHC monomer production and generation of specific pMHC multimers

The production of MHC monomers was performed as previously described by Hadrup et al.²⁹ In brief, HLA-A*0201 and -B*0702 heavy chains and human β_2m light chain were expressed in bacterial BL21 (DE3) pLysS strain (Novagen, Cat# 69451) and purified as inclusion bodies. After solubilization, A*0201/B*0702 inclusion bodies were refolded with β_2m light chain and a UV-sensitive ligand,^{30,31} and the folded monomers were biotinylated with BirA biotin-protein ligase standard reaction kit (Avidity, 318 LLC-Aurora, Colorado) and purified using a size-exclusion column (Waters, BioSuite125, 13 μ m SEC 21.5 \times 300 mm) and HPLC (Waters 2489). Specific pMHC monomers were generated by UV-induced peptide exchange³⁰ and multimerized with fluorochrome-conjugated streptavidin or coupled to dextramer according to specific protocols.

Enrichment of pMHC-specific T cells by magnetic bead sorting

Cryopreserved PBMCs were thawed and washed in R10 media containing DNase (40 U/ml, Stem Cell Technologies, Cat#07900) before incubation with PE (phycoerythrin)-coupled pMHC multimers (0.1 mg of each specificity) for 1 h at 4°C. Hereafter, cells were washed twice in R10 and incubated 15 min at 4°C with anti-PE microbeads (Miltenyi Biotec, Cat#130-048-801). Cells were washed twice after incubation, resuspended in 0.5 mL RPMI with DNase and applied to magnetic separation columns (MS; Miltenyi Biotec; Cat#130-042-201) placed in a magnetic field of a magnetic-activated cell sorting (MACS) separator through a 30 μ m pre-separation filter. After washing, cells were flushed out in 2 mL X-vivo (Lonza, Cat#Be04-418Q), 5% human serum, 100 U/mL IL-2 (Proleukin; Novartis, Cat#200-02), 15 ng/mL IL-15 (Peprotech, Cat#200-15), centrifuged and resuspended in 200 μ L of the same media containing 5×10^4 feeder cells, prepared and irradiated from the negative fraction during separation and 5×10^3 anti-CD3/CD28-coated Dynabeads (Invitrogen, Cat#111.31.D). Enriched cells were cultured in 96-well plates for 2–3 weeks, with bi-weekly change of medium and analyzed by pMHC multimer-specific T cell detection methods.

pMHC-specific expansion of T cells

Cryopreserved PBMCs were thawed and washed in R10 media, resuspended and cultured in X-vivo + 5% human serum. Cells were stimulated twice a week with the given pMHC complex, IL-2 and IL-21, all co-complexed on a dextran molecule for expansion of specific T cell populations and analyzed after two weeks by combinatorial fluorescently-encoded pMHC multimers.

Detection of pMHC-specific T cells by combinatorial fluorescently-encoded MHC multimers

The combinatorial encoding method and gating strategy is described in detail by Andersen et al.³² Briefly, a UV exchange reaction was carried out for each selected HLA-A*0201/B*0702 peptide ligand, followed by multimerization on two different streptavidin-conjugated fluorochromes. Thus, each of the peptide specificities was assigned a unique two-color combination. Five different streptavidin-conjugated fluorochromes were used for detection of specific T cells in Patient cohort 1: PE (phycoerythrin, Biolegend, Cat#405203), APC (allophycocyanin, Biolegend, Cat#405207), PE-Cy7 (phycoerythrin-cyanin 7, Biolegend, Cat#405206), PE-CF594 (BD, Cat#562284), and BV421 (brilliant violet, Biolegend, Cat#405226). Nine streptavidin-conjugated fluorochromes were used for detection of specific T cells in Patient cohort 2 and Healthy Donor cohort 2: PE, APC, PE-Cy7, BV421, Q-dot 585 (quantum dot, Invitrogen: Q10111MP), Q-dot 605 (Invitrogen, Cat#Q10101MP), Q-dot 625 (Invitrogen, Cat#A10196), Q-dot655 (Invitrogen: Q10121MP) and Q-dot705 (Invitrogen, Cat#Q10161MP). Breast cancer and healthy donor PBMCs were stained with a panel of up to 36 combinatorially encoded pMHC-multimers at a time, followed by staining with an antibody mix consisting of either CD8-BV480 (BD, Cat#566121 (clone RPA-T8)) in Patient cohort 1 or CD8-PerCP (Invitrogen, Cat#MHCD0831) in Patient cohort 2 and Healthy Donor cohort 2, dump channel antibodies CD4-FITC (CD4- fluorescein isothiocyanate, BD, Cat#345768), CD14-FITC (BD, Cat#345784) CD19-FITC (BD, Cat#345776), CD16-FITC (BD, Cat#335035) and CD40-FITC (Bio-rad, Cat#MCA1590F), and the dead cell marker LIVE/DEAD Fixable Near-IR (Invitrogen, Cat#L10119). Multimer positive T cell responses were gated as single, live, CD8⁺, FITC⁻ (dump channel), multimer color 1⁺, multimer color 2⁺, and negative for the remaining multimer colors, and defined by a minimum of 10 dual color positive events.

Detection of pMHC-specific T cells by barcoding

DNA-barcoded pMHC multimers were used to screen for T cell recognition against 157 pMHC specificities in a single sample. The method is described in detail in Bentzen et al.²⁰ Briefly, a UV exchange reaction was carried out for each selected HLA-A*0201/B*0702 peptide ligand, as described above. Each generated pMHC complex was coupled to DNA barcode- and PE-labeled dextran backbones, so that each specific peptide was encoded by a unique DNA barcode. Breast cancer and healthy donor PBMCs were stained with a pool of all barcoded MHC-multimers and an antibody mix of CD8-BV480, dump channel antibodies CD4-FITC, CD14-FITC, CD19-FITC, CD16-FITC, and CD40-FITC,

and the dead cell marker LIVE/DEAD Fixable Near-IR. Multimer-specific T cells were then sorted as single, live, CD8⁺, FITC⁻ (dump channel), PE⁺ fraction of cells, pelleted by centrifugation and cryopreserved at -80°C. DNA barcodes were amplified from the cell pellet and from a stored aliquot of the pMHC multimer reagent pool (used as baseline for comparison) by PCR, purified with a QIAquick PCR Purification kit (Qiagen, Cat#28104) and sequenced (Sequetech) using an Ion Torrent PGM 316 or 318 chip (Life Technologies). Sequencing data were processed by the software package Barracoda, available online at www.cbs.dtu.dk/services/barracoda. This tool identifies barcodes used in a given experiment, assigns sample ID and pMHC specificity to each barcode, and counts the total number of reads and clonally-reduced reads for each pMHC-associated DNA barcode. Log₂ fold changes in read counts mapped to a given sample relative to the mean read counts mapped to triplicate baseline samples are estimated with normalization factors determined by the trimmed mean of M-values method. False-discovery rates (FDRs) were estimated using the Benjamini-Hochberg method. A *p*-value is calculated based on the Log₂ fold change distribution, determining the strength of the signal compared to the input. Also, *p* < 0.001, corresponding to FDR < 0.1%, is established as the significance level determining a T cell response.

Functional assessment of pMHC-specific T cells by barcoding and intracellular flow cytometry

The functionality of pMHC-specific T cells was tested by combining intracellular cytokine staining (ICS) with a DNA barcode-based pMHC multimer staining, as previously described in Bentzen et al.²⁰ Briefly, patient-derived PBMCs were stimulated with either pre-stimulated IFN γ (PreproTech, Cat#300-02) breast cancer cell lines at a 10:1 ratio (PBMCs:cell lines), a pool of peptides with known reactivity in the specific patient or a leucocyte activation cocktail (LAC, BD, Cat#550583) positive control for 4 h at 37°C. After stimulation, cells were stained with barcoded MHC multimers, followed by staining with extracellular surface antibodies: CD3-FITC (BD, Cat#345763), CD8-BV480, and dead cell marker LIVE/DEAD Fixable Near-IR. Hereafter cells were permeabilized with the Intracellular Fix and Perm kit (eBioscience, Cat#88-8824-00), stained with intracellular antibodies TNF α -PE-Cy7 (BioLegend, Cat#502930) and IFN γ -APC (BD, Cat#341117), and fixated in 1% PFA until analysis.

Flow cytometry

All flow cytometry experiments were carried out on LSRII, Fortessa, and AriaFusion instruments (BD Biosciences). Data were analyzed in FACSDiva Software version 8.0.2 (BD Biosciences) and FlowJo version 10.4.2 (TreeStar, Inc.)

Statistical analyses

GraphPad Prism 7 for Mac OS X was used for graphing, statistical analyses and tools. This study included the D'agostino-Pearson omnibus normality test, unpaired parametric T-test

(following log-transformation to reach Gaussian distribution as needed), nonparametric Mann-Whitney test, Fischer's exact test, and Pearson's correlation coefficient.

Acknowledgments

We would like to thank all breast cancer patients and healthy donors for contributing blood samples to this study; Tina Seremet, Bente Rotbøl, Tripti Tamhane, Anna Gyllenberg Burkal, and Julien Candrian for excellent technical assistance, as well as all current and former members of the SRH group for scientific discussions.



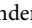

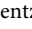
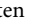
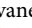

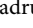
Disclosure of interest

The authors declare no potential conflicts of interest.

Funding

This research was funded in part through the Independent Research fund Danmarks Frie Forskningsfond (DK) (Grant no. DFF – 4004-00422) and the European Research Council, StG 677268 NextDART.

ORCID

Nadia Viborg  <http://orcid.org/0000-0001-9471-0895>
 Sofie Ramskov  <http://orcid.org/0000-0001-9413-8673>
 Rikke Sick Andersen  <http://orcid.org/0000-0001-7237-2215>
 Tim Fugmann  <http://orcid.org/0000-0002-7447-7480>
 Amalie Kai Bentzen  <http://orcid.org/0000-0002-5184-3054>
 Per thor Straten  <http://orcid.org/0000-0002-4731-4969>
 Inge Marie Svane  <http://orcid.org/0000-0002-9451-6037>
 Özcan Met  <http://orcid.org/0000-0002-3256-7592>
 Sine Reker Hadrup  <http://orcid.org/0000-0002-5937-4344>

References

- Bray F, Ferlay J, Soerjomataram I, Siegel RL, Torre LA, Jemal A. Global cancer statistics 2018: GLOBOCAN estimates of incidence and mortality worldwide for 36 cancers in 185 countries. *CA Cancer J Clin.* 2018;68:394–424. doi:10.3322/caac.v68.6.
- Emens LA. Breast cancer immunotherapy: facts and hopes. *Clin Cancer Res.* 2018;24:511–520. doi:10.1158/1078-0432.CCR-16-3001.
- Nathan MR, Schmid P. The emerging world of breast cancer immunotherapy. *Breast.* 2017;37:200–206. doi:10.1016/j.breast.2017.05.013.
- Rooney MS, Shukla SA, Wu CJ, Getz G, Hacohen N. Molecular and genetic properties of tumors associated with local immune cytolytic activity. *Cell.* 2015;160:48–61. doi:10.1016/j.cell.2014.12.033.
- Brown SD, Warren RL, Gibb EA, Martin SD, Spinelli JJ, Nelson BH, Holt RA. Neo-antigens predicted by tumor genome meta-analysis correlate with increased patient survival. *Genome Res.* 2014;24:743–750. doi:10.1101/gr.165985.113.
- Mcgranahan N, Furness AJS, Rosenthal R, Ramskov S, Lyngaa R, Saini SK, Jamal-Hanjani M, Wilson GA, Birkbak NJ, Hiley CT, et al. Clonal neoantigens elicit T cell immunoreactivity and sensitivity to immune checkpoint blockade. *Science.* 2016;351:1463–1469. doi:10.1126/science.aaf1490.
- Alexandrov LB, Nik-Zainal S, Wedge DC, Aparicio SAJR, Behjati S, Biankin AV, Bignell GR, Bolli N, Borg A, Børresen-Dale A-L, et al. Signatures of mutational processes in human cancer. *Nature.* 2013;500:415–421. doi:10.1038/nature12477.
- Zacharakis N, Chinnasamy H, Black M, Xu H, Lu Y-C, Zheng Z, Pasetto A, Langhan M, Shelton T, Prickett T, et al. Immune recognition of somatic mutations leading to complete durable regression in metastatic breast cancer. *Nat Med.* 2018;24:724–730. doi:10.1038/s41591-018-0040-8.
- Bjoern J, Lyngaa R, Andersen R, Hölmich LR, Hadrup SR, Donia M, Svane IM. Influence of ipilimumab on expanded tumour derived T cells from patients with metastatic melanoma. *Oncotarget.* 2017;8:27062–27074. doi:10.18632/oncotarget.v8i16.
- Krishnamurti U, Silverman J. HER2 in breast cancer: a review and update. *Adv Anat Pathol.* 2014;21:100–107. doi:10.1097/PAP.0000000000000015.
- Nath S, Mukherjee P. MUC1: A multifaceted oncoprotein with a key role in cancer progression. *Trends Mol Med.* 2014;20:332–342. doi:10.1016/j.molmed.2014.02.007.
- Bulun SE, Chen D, Lu M, Zhao H, Cheng Y, Demura M, Yilmaz B, Martin R, Utsunomiya H, Thung S, et al. Aromatase excess in cancers of breast, endometrium and ovary. *J Steroid Biochem Mol Biol.* 2007;106:81–96. doi:10.1016/j.jsbmb.2007.05.027.
- Bulun SE, Lin Z, Imir G, Amin S, Demura M, Yilmaz B, Martin R, Utsunomiya H, Thung S, Gurates B, et al. Regulation of aromatase expression in estrogen-responsive breast and uterine disease: from bench to treatment. *Pharmacol Rev.* 2005;57:359–383. doi:10.1124/pr.57.3.6.
- McHale K, Tomaszewski JE, Puthiyaveettil R, Livolsi VA, Clevenger CV. Altered expression of prolactin receptor-associated signaling proteins in human breast carcinoma. *Mod Pathol.* 2008;21:565–571. doi:10.1038/modpathol.2008.7.
- Gill S, Peston D, Vonderhaar BK, Shousha S. Expression of prolactin receptors in normal, benign, and malignant breast tissue: an immunohistological study. *J Clin Pathol.* 2001;54:956–960. doi:10.1136/jcp.54.12.956.
- Harada N. Aberrant expression of aromatase in breast cancer tissues. *J Steroid Biochem Mol Biol.* 1997;61:175–184. doi:10.1016/S0960-0760(97)80010-6.
- Speiser DE, Baumgaertner P, Voelter V, Devevre E, Barbey C, Rufer N, Romero P. Unmodified self antigen triggers human CD8 T cells with stronger tumor reactivity than altered antigen. *PNAS.* 2008;105:3849–3854. doi:10.1073/pnas.0800080105.
- Lesterhuis WJ, Schreiber G, Scharenborg NM, Brouwer HM-LH, Gerritsen M-JP, Croockewit S, Coulie PG, Torensma R, Adema GJ, Figdor CG, et al. Wild-type and modified gp100 peptide-pulsed dendritic cell vaccination of advanced melanoma patients can lead to long-term clinical responses independent of the peptide used. *Cancer Immunol Immunother.* 2011;60:249–260. doi:10.1007/s00262-010-0942-x.
- Rodenko B, Toebes M, Hadrup SR, van Esch WJE, Molenaar AM, Schumacher TNM, Ovaas H. Generation of peptide-MHC class I complexes through UV-mediated ligand exchange. *Nat Protoc.* 2006;1:1120–1132. doi:10.1038/nprot.2006.121.
- Bentzen AK, Marquard AM, Lyngaa R, Saini SK, Ramskov S, Donia M, Such L, Furness AJS, McGranahan N, Rosenthal R, et al. Large-scale detection of antigen-specific T cells using peptide-MHC-I multimers labeled with DNA barcodes. *Nat Biotechnol.* 2016;34:1037–1045. doi:10.1038/nbt.3662.
- Pedersen NW, Holm A, Kristensen NP, Bjerregaard A-M, Bentzen AK, Marquard AM, Tamhane T, Burgdorf KS, Ullum H, Jennum P, et al. CD8+ T cells from patients with narcolepsy and healthy controls recognize hypocretin neuron-specific antigens. *Nat Commun.* 2019;10:1–12. doi:10.1038/s41467-019-08774-1.
- Mahmoud SMA, Paish EC, Powe DG, Macmillan RD, Grainge MJ, Lee AHS, Ellis IO, Green AR. Tumor-infiltrating CD8+ lymphocytes predict clinical outcome in breast cancer. *J Clin Oncol.* 2011;29:1949–1955. doi:10.1200/JCO.2010.30.5037.
- Savas P, Virassamy B, Ye C, Salim A, Mintoff CP, Caramia F, Salgado R, Byrne DJ, Teo ZL, Dushyanthen S, et al. Single-cell profiling of breast cancer T cells reveals a tissue-resident memory subset associated with improved prognosis. *Nat Med.* 2018;24:986–993. doi:10.1038/s41591-018-0078-7.
- Schmid P, Adams S, Rugo HS, Schneeweiss A, Barrios CH, Iwata H, Diéras V, Hegg R, Im S-A, Shaw Wright G, et al. Atezolizumab and nab-paclitaxel in advanced triple-negative breast cancer. *N Engl J Med.* 2018;379:2108–2121. doi:10.1056/NEJMoa1809615.

25. Rammensee H-G, Bachmann J, Emmerich NPN, Bachor OA, Stevanovic S. SYFPEITHI: database for MHC ligands and peptide motifs. *Immunogenetics*. 1999;50:213–219. doi:10.1007/s002510050595.
26. Lundegaard C, Lamberth K, Harndahl M, Buus S, Lund O, Nielsen M. NetMHC-3.0: accurate web accessible predictions of human, mouse and monkey MHC class I affinities for peptides of length 8–11. *Nucleic Acids Res*. 2008;36:509–512. doi:10.1093/nar/gkn202.
27. Jurtz V, Paul S, Andreatta M, Marcatili P, Peters B, Nielsen M. NetMHCpan-4.0: improved peptide–MHC class I interaction predictions integrating eluted ligand and peptide binding affinity data. *J Immunol*. 2017;199:3360–3368. doi:10.4049/jimmunol.1700893.
28. Nielsen M, Lundegaard C, Blicher T, Lamberth K, Harndahl M, Justesen S, Røder G, Peters B, Sette A, Lund O, et al. NetMHCpan, a method for quantitative predictions of peptide binding to any HLA-A and -B locus protein of known sequence. *PLoS One*. 2007;2:e796. doi:10.1371/journal.pone.0000796.
29. Hadrup SR, Toebes M, Rodenko B, Bakker AH, Egan DA, Ovaa H, Schumacher TN. High-throughput T-cell epitope discovery through MHC peptide exchange. *Methods Mol Biol*. 2009;524:383–405.
30. Toebes M, Coccorsis M, Bins A, Rodenko B, Gomez R, Nieuwkoop NJ, van de Kastele W, Rimmelzwaan GF, Haanen JBAG, Ovaa H, et al. Design and use of conditional MHC class I ligands. *Nat Med*. 2006;12:246–251. doi:10.1038/nm1360.
31. Bakker AH, Hoppes R, Linnemann C, Toebes M, Rodenko B, Berkers CR, Hadrup SR, van Esch WJE, Heemskerk MHM, Ovaa H, et al. Conditional MHC class I ligands and peptide exchange technology for the human MHC gene products HLA-A1, -A3, -A11, and -B7. *PNAS*. 2008;105:3825–3830. doi:10.1073/pnas.0709717105.
32. Andersen RS, Kvistborg P, Frøsig TM, Pedersen NW, Lyngaa R, Bakker AH, Shu CJ, Straten PT, Schumacher TN, Hadrup SR. Parallel detection of antigen-specific T cell responses by combinatorial encoding of MHC multimers. *Nat Protoc*. 2012;7:891–902. doi:10.1038/nprot.2012.037.